MOLECULAR ECOLOGY

Molecular Ecology (2015) **24**, 4866–4885 doi: 10.1111/mec.13371

Seascape drivers of *Macrocystis pyrifera* population genetic structure in the northeast Pacific

MATTIAS L. JOHANSSON,*† FILIPE ALBERTO,* DANIEL C. REED,‡ PETER T. RAIMONDI,§ NELSON C. COELHO,* MARY A. YOUNG,§ PATRICK T. DRAKE,¶ CHRISTOPHER A. EDWARDS,¶ KYLE CAVANAUGH,** JORGE ASSIS,†† LYDIA B. LADAH,‡‡ TOM W. BELL,§§ JAMES A. COYER,¶¶ DAVID A. SIEGEL§§ and ESTER A. SERRÃO††

*Department of Biological Sciences, University of Wisconsin – Milwaukee, PO Box 413, Milwaukee, WI 53201, USA, †Great Lakes Institute for Environmental Research, University of Windsor, Windsor ON N9B 3P4, Canada, ‡Marine Science Institute, University of California, Santa Barbara, CA 93106, USA, §Department of Ecology and Evolutionary Biology, University of California, Santa Cruz, CA 95064, USA, ¶Ocean Sciences Department, University of California, Santa Cruz, CA 95064, USA, **Department of Geography, University of California, Los Angeles, CA 90095, USA, ††Center of Marine Sciences, University of Algarve, Campus de Gambelas, 8005-139 Faro, Portugal, ‡‡Department of Biological Oceanography, CISESE, Ensenada, C.P. 22860, Baja California, México, §§Earth Research Institute, University of California, Santa Barbara, CA 93106, USA, ¶¶Shoals Marine Laboratory, Cornell University, Portsmouth, NH 03801, USA

Abstract

At small spatial and temporal scales, genetic differentiation is largely controlled by constraints on gene flow, while genetic diversity across a species' distribution is shaped on longer temporal and spatial scales. We assess the hypothesis that oceanographic transport and other seascape features explain different scales of genetic structure of giant kelp, *Macrocystis pyrifera*. We followed a hierarchical approach to perform a microsatellite-based analysis of genetic differentiation in *Macrocystis* across its distribution in the northeast Pacific. We used seascape genetic approaches to identify large-scale biogeographic population clusters and investigate whether they could be explained by oceanographic transport and other environmental drivers. We then modelled population genetic differentiation within clusters as a function of oceanographic transport and other environmental factors. Five geographic clusters were identified: Alaska/Canada, central California, continental Santa Barbara, California Channel Islands and mainland southern California/Baja California peninsula. The strongest break occurred between central and southern California, with mainland Santa Barbara sites forming a transition zone between the two. Breaks between clusters corresponded approximately to previously identified biogeographic breaks, but were not solely explained by oceanographic transport. An isolation-by-environment (IBE) pattern was observed where the northern and southern Channel Islands clustered together, but not with closer mainland sites, despite the greater distance between them. The strongest environmental association with this IBE pattern was observed with light extinction coefficient, which extends suitable habitat to deeper areas. Within clusters, we found support for previous results showing that oceanographic connectivity plays an important role in the population genetic structure of *Macrocystis* in the Northern hemisphere.

Keywords: giant kelp, Lagrangian particle simulation, landscape genetics, marine connectivity, microsatellites, spatial genetic structure

Received 8 July 2015; revision received 26 August 2015; accepted 1 September 2015

Correspondence: Filipe Alberto, Fax: +1 414 229 3926; E-mail: albertof@uwm.edu

© 2015 John Wiley & Sons Ltd

Introduction

The development of genetic differentiation at relatively small spatial and temporal scales is largely controlled by constraints on gene flow, whereas genetic diversity across a species' distribution is shaped by processes working on longer temporal and spatial scales (Avise 2004; Templeton 2006). At small spatial scales and shorter coalescent times between populations, studying dispersal can tell us about present population connectivity (Rousset 1997, 2000; Hardy & Vekemans 1999) and its role in population dynamics (Castorani *et al.* in press). As the scales of spatial and temporal separation increase, migration over one or a few generations no longer explains the patterns observed. In fact, analyses at broader spatial and temporal scales often show that populations across the distribution range can be organized into different groups or clusters that are characterized by their genetic coancestry (Pritchard *et al.* 2000; Waples & Gaggiotti 2006). Genetically distinct biogeographic clusters of populations may have originated due to past disjunct distributions and rare gene flow caused by range contractions and extensions, dispersal barriers or vicariance, maintained by presently limited gene flow (Maggs *et al.* 2008; Assis *et al.* 2014). Moreover, these clusters may also represent units under differential local selection, a topic that has received increased attention recently with the advent of population genomics (Luikart *et al.* 2003).

Each genetic cluster identified at the biogeographic level is an individual spatial unit with shorter coalescence time and where ongoing connectivity may still be inferred in a meaningful way (Rousset 2007). At this level, the factors explaining population connectivity within different genetic clusters might differ, given the potential biotic and abiotic variability across a species' distribution range. The identity and role of these abiotic and biotic causes of genetic differentiation has been estimated using different statistical models to evaluate their fit as predictors of some measure of genetic differentiation (Balkenhol *et al.* 2009; Alberto *et al.* 2010, 2011; White *et al.* 2010). Because different spatial scales of genetic structure may be shaped by distinct processes acting at contrasting temporal scales, genetic clusters should ideally be identified prior to population connectivity analysis. Initial identification of genetic clusters allows the scale of impact of ecological processes to be correctly modelled. However, population genetic analysis is often conducted within a limited spatial scale, without model generalization to other unsampled range areas. The alternative problem, which is also quite common, is that range areas are analysed that extend across multiple genetic coancestry clusters, potentially leading to incorrect conclusions (Selkoe & Toonen 2011; Keller *et al.* 2013).

The most basic approach to studying population genetic connectivity over distance has been to assume that gene flow decreases linearly (or logarithmically for nonlinear 2D distributions, Rousset 1997) with Euclidean distance (isolation-by-distance, IBD, or stepping-stone model; Wright 1943; Slatkin 1993; Rousset 1997; Bohonak 1999). Under the stepping-stone model, we expect to find a positive linear relationship as pairwise genetic differentiation increases with the distance between two populations along linear distributions such as marine coastlines. However, this relationship saturates as a function of mean dispersal distance over all recruits (Rousset 1997, 2004; Selkoe & Toonen 2011) as dispersal between populations becomes negligible and drift becomes the primary genetic force structuring local allele frequencies (Hutchison & Templeton 1999; Keller *et al.* 2013). If this saturation point is not recognized and IBD slope is estimated from all points and distances, then the slope is likely to be incorrectly estimated. Because the focus of many studies is on testing whether the IBD slope is significantly >0 rather than on estimating an accurate slope or mean dispersal distance, the vast majority of IBD studies fit a single slope to all points. This probably leads many researchers to fail to detect genetic structure and may lead to overestimation of population connectivity in many marine species (Selkoe & Toonen 2011).

Once an appropriate IBD sampling scale is identified, another approach to discern connectivity in marine organisms is the use of high-resolution biophysical models to estimate planktonic dispersal (Cowen & Sponaugle 2009). These models can provide connectivity measurements for IBD-type genetic models by simulating the release of large numbers of propagules, allowing estimation of mean connectivity between locations (Alberto *et al.* 2011; Treml *et al.* 2012; Riginos & Liggins 2013). This connectivity is usually a time-based metric, for example the mean time it takes a propagule to move from location i to j. Additionally, these models can incorporate seasonal and interannual variability in environmental factors, such as current strength, to account for actual spatiotemporal variability in connectivity between populations (Cowen & Sponaugle 2009; Mitarai *et al.* 2009). Furthermore, by taking into account the directionality of ocean currents, they estimate the asymmetry in larval transport between population pairs, which is not possible using any distance-based approach. In several cases, such time-based measures of oceanographic connectivity have been shown to be more effective than traditional distance-based approaches at predicting genetic differentiation in marine systems (Selkoe *et al.* 2007, 2010; White *et al.* 2010; Alberto *et al.* 2011; Assis *et al.* 2015). This approach is

© 2015 John Wiley & Sons Ltd

one of a suite of newer approaches collectively termed 'seascape genetics' that, like landscape genetics in terrestrial systems, take into account both biotic and abiotic landscape features that affect population connectivity (Riginos & Liggins 2013).

Landscape genetics is primarily distinguished from classical population genetics by the idea that the quality and quantity of unsuitable habitat areas between patches of more favourable habitat are the primary driver of population structure, rather than (or in addition to) linear distance (Holderegger & Wagner 2008; Selkoe *et al.* 2008, 2010). Compared to the large body of work in terrestrial systems, relatively few studies have incorporated characteristics of habitat and nonhabitat areas into research on gene flow in marine systems, presumably because of the inherent difficulty in mapping and characterizing marine habitats in any detail. However, a small but growing body of work has begun to relate genetic connectivity measures and seascape characteristics such as habitat discontinuities (Johansson *et al.* 2008; Alberto *et al.* 2010; D'Aloia *et al.* 2014), bathymetry (Hyde *et al.* 2008), sea surface temperature (Jørgensen *et al.* 2005; Amaral *et al.* 2012; Eberl *et al.* 2013), salinity (Jørgensen *et al.* 2005), coastal pollution (Puritz & Toonen 2011) and oceanographic transport at large (Galindo *et al.* 2006; Coleman *et al.* 2011) and small scales (Gilg & Hilbish 2003; Alberto *et al.* 2011; López-Duarte *et al.* 2012; Coscia *et al.* 2013).

Patterns of biogeography, like those of population connectivity, are driven by characteristics of the landscape and environment, although formed over longer temporal scales. One approach to identify potential population genetic breaks has been to look for features that explain biogeographic breaks (Avise 1992). For example, in a global-scale study of bivalve biogeography, Belanger *et al.* (2012) demonstrated that the large-scale biogeographic structure of shallow-marine bivalve faunas can be predicted with 89-100% accuracy from data on sea surface temperature, salinity and productivity. In brown algae, large-scale biogeographic structure typically coincides with variation in distributional patterns that is mainly explained by variation in temperature limits and several other factors (Assis *et al.* 2014; Neiva *et al.* 2014).

A well-known biogeographic break has been described between southern and central California, in the area of Point Conception (at 34°26′54″ N 120°28′19″ W, Fig. 1), where the Californian biogeographic province meets the Oregonian, and where a number of species have their range endpoints (Valentine 1966; Briggs 1974; Newman 1979; Doyle 1985; Burton 1998). This boundary is characterized by a 5 °C north-to-south temperature gradient, driven by the interaction between the southward-flowing California Current and the north- and westward-flowing nearshore components of the southern California Eddy, along with shifts in upwelling and other related environmental parameters, such as dissolved oxygen, salinity and nutrient availability (Burton 1998; Eberl *et al.* 2013).

The distribution range of our model species, the giant kelp (*Macrocystis pyrifera*, hereafter *Macrocystis*, as the genus is monospecific; Coyer *et al.* 2001; Demes *et al.* 2009; Macaya & Zuccarello 2010a), spans the region of biogeographic change from central to southern California. Therefore, we expect the factors driving the biogeographic change to also impact the phylogeography of giant kelp. Numerous factors influence the distribution, survival and growth of *Macrocystis*, including substratum type, sedimentation rate, irradiance, current flows, wave exposure, temperature, stratification, nutrient concentrations, grazing, competition, disease and pollution (Schiel & Foster 2015). Previous research on *Macrocystis* biogeography at the large spatial scale (global: Coyer *et al.* 2001; Macaya & Zuccarello 2010a; regional: Macaya & Zuccarello 2010b) suggested that dispersal was possible between the Northern hemisphere and the Southern hemisphere during the last glacial maximum and that phylogeographic breaks in *Macrocystis* in the southeastern Pacific correspond approximately to known biogeographic breaks. However, these studies were limited by the low resolution of the markers used (rDNA, mitochondrial DNA). Microsatellite markers, with their high level of polymorphism, offer the potential to look at much finer-scale biogeographic structure within a region.

In two earlier studies, we related pairwise genetic distance (estimated using microsatellite markers) to habitat continuity and geographic distance (stepping-stone model, Alberto *et al.* 2010) or to habitat continuity and oceanographic spore transport time (seascape model, Alberto *et al.* 2011) along the mainland coast of the Santa Barbara Channel. In this study, we move beyond this scale to identify population clusters of *Macrocystis* in the northeast Pacific, test the null hypothesis that these clusters are a function of oceanographic connectivity, and search for potential environmental drivers of this clustering. Within each identified cluster, we test the generality of our previously published models of the relationship between oceanography, distance and habitat continuity in driving the population genetic structure of giant kelp outside the Santa Barbara Channel. Finally, we investigate the associations between genetic differentiation and previously untested environmental drivers, such as sea surface temperature and wave exposure. Our goal is to integrate the biological and physical processes that drive the patterns of population connectivity in *Macrocystis* to obtain a more complete understanding of genetic connectivity in marine coastal populations.

© 2015 John Wiley & Sons Ltd

Materials and methods

Macrocystis life history

Found worldwide in the eastern Pacific and Southern Ocean, *Macrocystis pyrifera* is the most widespread kelp species and the largest alga in the world (Graham *et al.* 2007; Schiel & Foster 2015). Although *Macrocystis* is found in the northeast Pacific as far north as Alaska, and as far south as Punta San Hipolito, Baja California Sur, Mexico, its dominance decreases dramatically north of Monterey Bay, California (Foster & Schiel 1985). Thus, we focused our analyses primarily on populations south of Monterey Bay; we include four additional locations (Canada and Alaska) to represent the disjunct northern distribution.

The haplodiplontic kelp life history consists of a macroscopic, diploid sporophyte that produces haploid male and female spores via meiosis; these originate free-living microscopic male and female gametophytes that produce gametes. Dispersal is primarily via the transport of spores, which can survive up to 1 week in the plankton and disperse distances up to tens of kilometres, although most settle closer (Reed *et al.* 1992; Gaylord *et al.* 2002). In *Macrocystis*, additional (and potentially longer distance) dispersal may occur as a result of the transport of dislodged fertile sporophytes by ocean currents (Hobday 2000; Hernández-Carmona *et al.* 2006; Saunders 2014), although the spore contribution of drifting sporophytes has not been shown to be ecologically meaningful (Reed *et al.* 2004). After dispersing, spores settle to the seabed and germinate into male and female gametophytes, which subsequently produce gametes. Fertilization occurs on the female gametophyte and involves short-range dispersal of the sperm. In contrast to many marine organisms, fertilization occurs after dispersal, and sporophyte recruitment is therefore limited to areas of relatively dense spore settlement because fertilization requires male and female gametophytes to be present in sufficient densities (>1 mm^{-2}) for the sperm to detect a pheromone released by the egg, triggering release and attraction (Boland *et al.* 1983; Reed *et al.* 1991). After fertilization, significant density-dependent mortality of early life stages leads to the adult densities typically seen in the field (Johansson *et al.* 2013).

Sample collections

Tissue samples were obtained from blades of *Macrocystis* collected at 62 sites (hereafter referred to as populations) ranging from Sitka, Alaska, USA, to Bahia Tortugas, Baja California Sur, Mexico, along the Pacific coast of North America (Fig. 1, Table 1). A single blade was haphazardly collected by divers from ~50 different individuals (separated by at least 2 m) from each population (n = 2631 total blades collected). A 2-cm^2 piece was excised from each blade and dried in silica gel desiccant for DNA extraction.

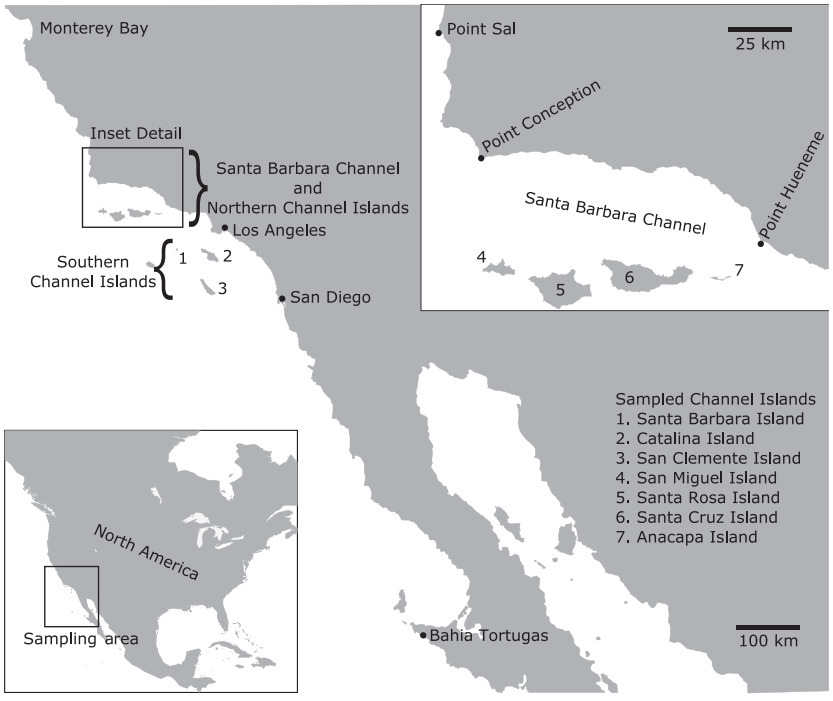

Fig. 1 Map showing sampling region in the eastern North Pacific. Key locations discussed in the manuscript are indicated.

© 2015 John Wiley & Sons Ltd

Table 1 Population genetics summary statistics by sampled population of *Macrocystis pyrifera*

Population (Code)	Latitude	Longitude	*n*	A_R	H_E	H_O	F_{IS}	*P*
Sitka, Alaska (NS1)	57°2′30.23″ N	135°20′52.25″ W	30	3.27	0.415	0.415	−0.254	0.998
Craig, Alaska (NC1)	55°28′11.61″ N	133°11′26.75″ W	29	2.21	0.201	0.237	−0.514	1.000
Nuchatlitz, Canada (CND)	49°36′57.13″ N	126°32′17.16″ W	25	1.94	0.125	0.137	−0.156	0.936
Bamfield Island, Canada (BAM)	48°50′22.98″ N	125°8′30.13″ W	39	1.85	0.256	0.229	−0.252	0.996
Sandhill Bluff (SHB)	36°58′27.30″ N	122°9′6.78″ W	40	4.26	0.536	0.567	−0.082	0.953
Terrace Point (TPO)	36°56′45.12″ N	122°3′46.74″ W	37	3.71	0.494	0.506	−0.024	0.699
Asilomar (ASI)	36°37′56.10″ N	121°56′48.06″ W	40	5.11	0.647	0.638	−0.001	0.576
Stillwater Cove (SWC)	36°33′13.26″ N	121°56′24.12″ W	37	5.25	0.622	0.640	−0.027	0.761
Esalen (ESL)	36°7′48.72″ N	121°39′10.44″ W	32	4.85	0.619	0.642	−0.069	0.918
La Cruz (LCR)	35°42′48.66″ N	121°19′36.06″ W	19	5.53	0.632	0.615	−0.005	0.552
Cayucos (CAY)	35°34′9.60″ N	121°7′18.96″ W	40	4.99	0.625	0.608	0.051	0.127
Estero (EST)	35°28′27.72″ N	121°1′37.62″ W	39	5.36	0.634	0.622	0.043	0.175
Montana de Oro (MDO)	35°13′59.64″ N	120°53′26.88″ W	41	5.42	0.618	0.533	0.121	0.007
Avila (AVL)	35°10′2.28″ N	120°42′46.38″ W	52	4.81	0.606	0.574	0.040	0.213
Purisma (PUR)	34°43′48.30″ N	120°37′34.32″ W	50	5.37	0.577	0.514	0.070	0.056
Arguello (ARG)	34°32′48.66″ N	120°36′31.80″ W	16	6.18	0.612	0.641	−0.162	0.974
Jalama (JAL)	34°28′25.86″ N	120°29′9.78″ W	49	5.77	0.629	0.602	0.025	0.288
Cojo (COJ)	34°26′35.58″ N	120°25′20.40″ W	44	7.07	0.685	0.666	0.007	0.451
Bulito (BUL)	34°27′31.98″ N	120°20′0.36″ W	51	6.38	0.687	0.640	0.084	0.008
Arroyo Hondo (AHO)	34°28′18.72″ N	120°8′39.78″ W	31	7.04	0.674	0.608	0.062	0.101
Arroyo Quemado (AQU)	34°28′7.62″ N	120°7′17.10″ W	50	6.63	0.709	0.682	0.065	0.036
Naples Reef (NAP)	34°25′20.40″ N	119°57′10.56″ W	48	7.21	0.722	0.647	0.083	0.011
Isla Vista (IVI)	34°24′10.20″ N	119°51′28.32″ W	50	7.18	0.719	0.679	0.035	0.182
Goleta Bay (GOL)	34°24′49.62″ N	119°49′20.64″ W	46	6.75	0.711	0.577	0.223	<0.001*
Arroyo Burro (ABU)	34°24′0.42″ N	119°44′39.78″ W	36	6.24	0.694	0.642	0.063	0.098
Mohawk (MOH)	34°23′39.60″ N	119°43′48.00″ W	44	6.99	0.737	0.695	0.046	0.125
Carpinteria (CAR)	34°23′32.70″ N	119°32′37.68″ W	50	6.80	0.686	0.680	0.018	0.313
Emma Wood (EWO)	34°17′26.15″ N	119°20′32.46″ W	33	6.33	0.665	0.603	0.052	0.159
San Miguel Island NW (MNW)	34°2′20.22″ N	120°26′30.96″ W	41	7.19	0.675	0.664	−0.052	0.920
San Miguel Island SW (MSW)	34°2′39.12″ N	120°19′30.60″ W	40	7.37	0.687	0.669	−0.040	0.857
San Miguel Island SE (MSE)	34°1′41.94″ N	120°23′57.12″ W	46	8.06	0.751	0.704	0.010	0.416
San Miguel Island NE (MNE)	34°1′4.50″ N	120°20′2.46″ W	48	7.90	0.736	0.705	−0.038	0.857
Santa Rosa Island SW (RSW)	33°57′48.54″ N	120°12′42.84″ W	48	9.23	0.774	0.711	0.083	0.003
Santa Rosa Island NW (RNW)	34°0′34.92″ N	120°11′16.92″ W	50	9.03	0.760	0.691	0.040	0.097
Santa Rosa Island NE (RNE)	33°59′37.68″ N	120°2′15.30″ W	49	8.95	0.774	0.697	0.097	0.001
Santa Rosa Island SE (RSE)	33°55′50.16″ N	120°1′12.96″ W	46	8.56	0.772	0.678	0.062	0.059
Santa Cruz Island NW (CNW)	34°3′24.36″ N	119°45′17.94″ W	48	8.24	0.768	0.642	0.131	<0.001*
Santa Cruz Island SE (CSE)	34°0′16.92″ N	119°32′47.22″ W	53	8.89	0.797	0.688	0.117	<0.001*
Santa Cruz Island NE (CNE)	34°2′46.68″ N	119°32′49.14″ W	52	8.49	0.769	0.769	0.124	<0.001*
Anacapa Island SW (ASW)	34°0′52.20″ N	119°25′13.02″ W	49	9.21	0.794	0.743	0.067	0.011
Anacapa Island NW (ANW)	34°0′16.02″ N	119°25′10.74″ W	52	9.70	0.810	0.734	0.095	<0.001*
Anacapa Island NE (ANE)	34°0′56.28″ N	119°22′13.98″ W	53	9.04	0.801	0.704	0.136	<0.001*
Anacapa Island SE (ASE)	34°0′49.86″ N	119°21′38.34″ W	53	8.47	0.774	0.670	0.144	<0.001*
Leo Carillo (LCA)	34°2′34.56″ N	118°56′4.20″ W	27	8.07	0.784	0.637	0.128	0.003
Palos Verdes (PVE)	33°48′13.02″ N	118°23′46.20″ W	33	8.29	0.788	0.681	0.053	0.115
Santa Barbara Island (SBI)	33°29′21.55″ N	119° 1′43.67″ W	43	8.12	0.738	0.613	0.159	<0.001*
Catalina Island Backside 2 (CIR)	33°25′45.72″ N	118°31′49.32″ W	40	8.06	0.757	0.696	0.094	0.003
Catalina Island Backside 1 (CIB)	33°20′2.76″ N	118°29′16.68″ W	40	8.44	0.791	0.738	0.074	0.011
Catalina Island Quarry (CIQ)	33°26′32.51″ N	118°28′20.88″ W	42	7.51	0.750	0.728	0.015	0.354
Catalina Island Little Gibraltar (CLG)	33°25′21.42″ N	118°24′39.84″ W	40	7.76	0.782	0.746	0.022	0.296
San Mateo (SMA)	33°22′4.00″ N	117°35′24.40″ W	40	8.12	0.780	0.755	−0.020	0.764
San Clemente Island South (SCS)	32°50′3.96″ N	118°28′21.60″ W	50	7.07	0.762	0.625	0.190	<0.001*
San Clemente Island North (SCN)	32°51′23.64″ N	118°23′19.02″ W	26	8.01	0.766	0.643	0.170	<0.001*
San Diego (SDI)	32°40′54.72″ N	117°15′42.12″ W	28	8.66	0.815	0.763	0.039	0.182
Punta San Miguel, Mexico (MXA)	31°54′0.06″ N	116°44′40.95″ W	48	8.57	0.817	0.739	0.017	0.330
Sauzal, Mexico (MXB)	31°53′0.55″ N	116°41′45.96″ W	48	8.75	0.806	0.772	0.014	0.364

© 2015 John Wiley & Sons Ltd

Table 1 *Continued*

Population (Code)	Latitude	Longitude	n	A_R	H_E	H_O	F_{IS}	P
Punta Morro, Mexico (MXD)	31°51′29.57″ N	116°40′26.36″ W	48	8.33	0.791	0.737	−0.015	0.718
Punta Banda, Mexico (PBB)	31°42′38.10″ N	116°41′43.44″ W	60	8.68	0.817	0.775	−0.006	0.642
Campo Kennedy, Mexico (MXE)	31°42′8.48″ N	116°41′1.29″ W	48	8.84	0.805	0.775	−0.006	0.611
Isla Natividad, Mexico (MXH)	27°51′15.53″ N	115°11′10.40″ W	48	7.69	0.758	0.686	−0.017	0.692
Punta Eugenia, Mexico (MXG)	27°51′2.75″ N	115° 4′45.49″ W	48	7.54	0.761	0.717	−0.014	0.675
Bahia Tortugas, Mexico (MXF)	27°39′21.41″ N	114°52′35.62″ W	48	6.81	0.705	0.627	0.046	0.149

n, sample size; A_R, standardized allelic richness, based on 15 samples; H_E, unbiased expected heterozygosity; H_O, observed heterozygosity; F_{IS}, inbreeding coefficient.
*Significant F_{IS} values at Bonferroni-corrected 0.05 level (P = 0.00093).

Genotyping

Genomic DNA was extracted from dried tissue samples using the NucleoSpin 96 Plant Kit II (Macherey-Nagel, Duren, Germany) and standard protocols. All individuals were genotyped at seven microsatellite loci (Mpy-8, Mpy-11, Mpy-14, BC-4, BC-18, BC-19, BC-25) using PCR conditions as described in Alberto *et al.* (2009). Fragment lengths were assayed on an ABI PRISM 3130XL DNA analyser (Applied Biosystems) using the GeneScan-500 LIZ standard (at the CCMAR genotyping platform). STRAND version 2.4.59 (Locke *et al.* 2000) was used to score raw allele sizes, which were subsequently binned into allele classes using the R package MSATALLELE (Alberto 2009) in R version 3.0.3 (R Development Core Team 2015).

Population genetics summary statistics

Allelic richness was estimated for a standardized sample of 15 individuals per population using the R package STANDARICH (Alberto *et al.* 2006). Observed and unbiased expected heterozygosity was calculated using GENETIX version 4.05.2 (Belkhir *et al.* 2004). The inbreeding coefficient (F_{IS}) was estimated using ARLEQUIN 3.5 (Excoffier & Lischer 2010) and tested for deviations from zero using a permutation test (1000 permutations) with significance values adjusted using the Bonferroni correction for multiple tests. As inbreeding coefficients were significant for several island and one mainland collection, we assessed the presence of null alleles using MICRO-CHECKER version 2.2.3 (Van Oosterhout *et al.* 2004). Null alleles were identified in several populations with significant F_{IS} values, so we used FREENA (Chapuis & Estoup 2007) to estimate genetic differentiation using standard F_{ST} as well as unbiased corrected F_{ST} 'excluding null alleles' (ENA) method. While uncorrected and ENA-corrected pairwise F_{ST} values were significantly different in a paired two-sample t-test (t = 16.86, P < 0.001), both measures of F_{ST} were highly correlated (Pearson correlation = 0.999) and the absolute difference in mean F_{ST} (0.002) is unlikely to be biologically meaningful. Therefore, we used uncorrected F_{ST} to describe genetic differentiation as a response in all the linear models described below (see within-cluster genetic differentiation).

Large spatial-scale genetic differentiation

We used the program STRUCTURE version 2.3.4 (Pritchard *et al.* 2000) to infer underlying population structure along the sampled giant kelp geographic range. All runs in STRUCTURE used the admixture model with allele frequencies correlated among populations, and with an initial burn-in of 250 000 steps and 750 000 collected data steps. We performed 10 independent runs per value of K (number of clusters), with K ranging from 1 to 11. The best-fitting number of populations was chosen based on the statistic ΔK (Evanno *et al.* 2005), and on visual inspection of the STRUCTURE barplots. Populations were assigned to clusters using mean individual proportions of ancestry (Q).

We used a network, built in R (R Development Core Team 2015) package IGRAPH (Csardi & Nepusz 2006), to represent the matrix of pairwise population genetic differences, estimated using Cavalli-Sforza and Edwards chord distance. To assess the relationships between the main genetic clusters in our study and visually identify the network best matching our STRUCTURE classification, the full network was pruned by sequentially removing edges (i.e. population pairwise links in the network) of decreasing genetic distance stopping at a point where the main groups of tightly connected sites still remained connected (i.e. avoiding the separation of any large network cluster from the main network). The number of network communities and the respective population classification was estimated at each step of the pruning process using the 'fastgreedy' community detection algorithm implemented in IGRAPH (Clauset *et al.* 2004; Blondel *et al.* 2008).

© 2015 John Wiley & Sons Ltd

To test the null hypothesis that clusters identified in STRUCTURE result from oceanographic connectivity, we estimated connectivity between all kelp-containing areas in the southern California Bight using an analysis of Lagrangian (water-following) particle simulations, described in Mitarai *et al.* (2009) and Simons *et al.* (2013). Briefly, monthly mean minimum transport times were calculated as the shortest probability-weighted mean transit time in days for Lagrangian particles travelling between a source and a destination location (see Mitarai *et al.* 2009 and Simons *et al.* 2013 for details of the Lagrangian particle simulations and Watson *et al.* 2011 and Alberto *et al.* 2011 for definition and application of monthly mean minimum times). Because genes are exchanged whenever propagules successfully migrate between populations, allele frequency divergence between two populations is expected to depend on the shortest transport time between them (Alberto *et al.* 2011). Locations in this analysis are the 118 (of 135) nearshore, ~10 km Regional Ocean Modeling System (ROMS; Shchepetkin & McWilliams 2005) patches shown to contain kelp by our 28-year Landsat 5 THEMATIC MAPPER database (Cavanaugh *et al.* 2011, 2014). Because this ROMS model does not extend into central California nor south of the United States–Mexico border, populations outside this region were excluded from this analysis.

Mean minimum transit times, estimated over annual and seasonal (spring, summer, fall and winter) timescales based upon 10 years of available ROMS simulations (January 1996–December 2006), were used to test the association of seasonal variation in ocean circulation with genetic clusters identified in STRUCTURE. We used IGRAPH to represent annual and seasonal oceanographic transport distances as networks, with network edges defined as transport times between population pairs. We used the IGRAPH 'fastgreedy' network community detection algorithm to group populations into different communities in each transport network and compared these communities to STRUCTURE assignment clusters. For each network, we started from the full graph (i.e. full pairwise matrix) and sequentially removed the edge corresponding to the longest remaining transport time until all edges were removed. At each iteration, we used the adjusted Rand index (Hubert & Arabie 1985) to calculate the similarity between population classifications into network communities and STRUCTURE clusters. The network pruning iteration with maximum adjusted Rand index was selected as the best agreement between each transport time network and STRUCTURE classification.

Additionally, to test for an isolation-by-environment (Wang & Bradburd 2014) pattern that could explain the genetic clusters estimated by STRUCTURE analysis, we ran a canonical correspondence analysis (CCA), in R package CCA (Gonzalez *et al.* 2008). The response variables were the *Q*-values for each site to belong to each of four genetic clusters (i.e. excluding Alaska/Canada sampling populations). The clusters used for these analyses were as follows: (i) central California (Terrace Point to Avila), (ii) Santa Barbara Channel (Purisma to Emma Wood), (iii) Channel Islands and (iv) the southern part of the southern California Bight and Punta Banda, in Baja California (the lack of environmental data precluded other populations in Baja California from being included in this analysis). The environmental predictor variables were based on site-specific values for sea surface temperature, significant wave height, light extinction coefficient, photosynthetically active radiation (PAR) and available light at the bottom. These variables were developed reflecting the long-term average and the extreme conditions, putatively acting on the physiology of *Macrocystis*, with different sources of data gridded from 2000 to 2010. The long-term average of sea surface temperature of the hottest summer months (JJAS) was produced using the Operational Sea Surface Temperature and Sea Ice Analysis (OSTIA; Donlon *et al.* 2012), a data set on a ~5-km resolution, which combines *in situ* measurements with data from the group for high-resolution sea surface temperature (GHRSST; Martin *et al.* 2007, 2012). The long-term average of significant wave height of the winter months (DJFM) with highest waves was produced using the European Centre for Medium-Range Weather Forecasts (Dee *et al.* 2011), a data set on a ~11.5-km resolution. The long-term average of light extinction coefficient (kd490) and PAR were obtained from the Group on Earth Observations System of Systems (GlobColour; http://hermes.acri.fr/), a data set merging MERIS, SeaWiFS, MODIS and VIIRS level-2, at a resolution of ~5 km. All environmental data were gridded to match the same 5-km resolution using bilinear interpolation. Site latitude and longitude were also included to control for the potential confounding effects of distance and spatial autocorrelation. We used a stepwise model-building approach in the R package vegan (Oksanen *et al.* 2015) to select the best model for the data and used variance partitioning to quantify the variation explained by the tested variables (Borcard *et al.* 1992; Økland & Eilertsen 1994).

Modeling within-cluster genetic differentiation

Using a multiple regression approach, we modelled how pairwise genetic differentiation was associated with different putative drivers of gene flow between giant kelp populations. Separate models were used within each of the genetic coancestry groups detected above, with the modification that the few mainland southern California sites for which we had environmental data (Leo Carrillo, LCA; Palos Verdes, PVE; San

© 2015 John Wiley & Sons Ltd

Mateo, SMA; San Diego, SDI) were combined with the Channel Island sites to make a single southern California group. The response variable, genetic differentiation, was pairwise $F_{ST}/(1 - F_{ST})$, and the predictor variables are described below.

Habitat continuity and geographic distance were characterized using a 28-year time series of kelp canopy biomass derived from Landsat 5 Thematic Mapper satellite imagery (Cavanaugh *et al.* 2011, 2014; Bell *et al.* 2015). We assembled a composite of Landsat pixels where kelp was quantified from 1984 to 2011 to represent the maximum areal extent of kelp habitat in central and southern California, following the methods in Cavanaugh *et al.* (2011). Using the Landsat database and the Cost Distance tool in ARCGIS (ESRI 2011), we created a matrix of shortest oceanic distances between all pairs of populations by masking habitat areas and calculating the shortest distance between locations that stayed within the mask. Distances to island sites took the shortest distance between masks (i.e. over open water) and then followed the mask to our sampling sites. We created a matrix of standardized habitat continuity using these pairwise distances and our composite habitat area (i.e. the total area of kelp along the track between populations) to calculate the area of habitat in square kilometres per kilometre of distance between all pairs of study populations.

Pairwise oceanographic transport time was estimated using the ROMS particle simulations, as described above for our cluster-based analysis. In this analysis, locations were limited to ROMS model cells containing our study sites. To facilitate comparisons with our previous results (Alberto *et al.* 2011), we limited the ROMS output used to transport occurring between January 1997 and December 2002 (7 years). This excluded sites in central California and most sites along the Baja California peninsula. We estimated annual, seasonal and monthly minimum transport times to test for associations between oceanographic connectivity and within-cluster genetic structure.

Central California sites are not included in the domain of the ROMS configuration described above, and water parcel connectivity was determined using an alternative simulation of the California Current System that extends from near the southern tip of Vancouver Island, Canada, to midway down the Baja California Peninsula at 1/30th degree horizontal resolution and 42 terrain-following levels (Drake *et al.* 2011). The Drake model differs from the Mitarai *et al.* (2009) model of the southern California Bight in several ways, extending over a greater geographical area but at lower grid resolution; as a result, it has significantly larger settlement and release cells between which transport time statistics were calculated (Drake: 40 km alongshore × 10 km offshore, Mitarai: 5 km radius), and does not resolve the circulation around the Channel Islands at as high resolution as the Mitarai model. Thus, our preference was to use both models for different sections of coast, as use of the Drake model for the whole sampling area would have resulted in the loss of significant numbers of sampling sites. The Drake model reasonably reproduced the overall spatial and temporal structure of the California Current System as well as statistics of energetic mesoscale and nearshore submesoscale variability (Drake *et al.* 2011, in press). In the model, virtual drifters representing kelp spores were released every other day during springtime (April–June) for 7 years (2000–2006) within near-coastal cells extending approximately 40 km alongshore and 10 km offshore and together blanketing the coast from Los Angeles, CA, to Oregon. The variable geometry of the coastline and bathymetry resulted in a variable number of floats being released in different nearshore cells (mean ≈ 120 per release per cell, SD ≈ 43 per release per cell). Modelled spores were released with approximately uniform spatial distribution within each cell and over the upper 20 m of the water column. Spores were transported by the full, 3-dimensional circulation, and their vertical position was influenced by modelled turbulent mixing as described in Drake *et al.* (2011, 2013). Transit times were defined as the minimum probability-weighted average time required for spores to travel between nearshore source and settlement cells (equation 13 in Mitarai *et al.* 2009; Drake *et al.* 2011).

For the within-cluster linear regression analysis, we derived pairwise statistics describing the difference in sea surface temperature and significant wave height between sites. Sea surface temperature data are 15-day averages at a 1-km spatial resolution from the Moderate Resolution Imaging Spectroradiometer (MODIS) instruments on the Terra and Aqua satellites (www.spg.ucsd.edu/Satellite_data/California_Current/) from 2000 to 2012. For each population, data were averaged across all years for a 'winter' semester (approximately December through May) and a 'summer' semester (approximately June through November) and absolute pairwise differences calculated between all populations. Significant wave height data for 1998–2012 came from the Coastal Data Information Program (CDIP, www.cdip.ucsd.edu). This model provides hourly estimates of significant wave height at a depth of 10 m at an 800-m spatial resolution. As with sea surface temperature, maximum significant wave height for each 15-day period was averaged across all years for winter and summer semesters and absolute pairwise differences calculated between populations.

We used a backward model selection approach, where predictor variables are eliminated one at a time

© 2015 John Wiley & Sons Ltd

with the predictor with the least significant partial regression slope (highest *P* value) eliminated at each step until all remaining variables are significant. The selected model was then compared with alternative models that replaced annual minimum transport time with seasonal and monthly minimum transport times, as well as single-predictor models for habitat continuity, geographic distance and the best-fitting minimum transport time. Finally, the goodness of fit of different models and optimized submodels was compared using the Bayesian information criterion (BIC).

Results

Population genetics summary statistics

Standardized allelic richness ranged from 1.85 to 9.70 alleles, at $n = 15$, with highest values in the northern Channel Islands, San Diego and northern Baja California and lower values in the extreme north (Fig. 2, Table 1). Observed heterozygosity varied from 0.137 to 0.775, while expected heterozygosity varied from 0.125 to 0.817 (Table 1). Estimated global F_{ST} was 0.121 (95% CI 0.09–0.157).

Large-scale genetic differentiation

STRUCTURE analysis with the complete data set identified a break between populations north and south of a parallel separating the Santa Barbara Channel coastal populations and the northern Channel Islands, intersecting the mainland coast south of the Emma Wood population (first seen in $K = 2$, Fig. 3A). From $K = 3$ to $K = 5$ (Fig. 3A), additional breaks appear between Avila and Purisma (north of Point Conception, at approximately 34°44′ N to 35°09′ N) separating most central California samples from southern California; in southern California separating Channel Island populations from the southern California mainland and Baja California peninsula populations; and between far northern populations (Alaska and Canada) and central California. Mapping $K = 5$ structure (Fig. 3B) shows that groups identified are geographically coherent, with admixture apparent in populations near transition zones. In most cases, assignment of populations to clusters was straightforward, with mean *Q* values over 60–70% for a single cluster. In two cases, Leo Carrillo (LCA) and Palos Verdes (PVE), assignments were more evenly mixed. These two populations fall within a transition zone between three different clusters, and *Q* values for all three clusters were below 50%. We assigned both transitional populations to the southern California mainland/Baja California peninsula cluster, which had the highest *Q* value (LCA: 43%, PVE: 46%), for environmental analysis. In summary, we identified five clusters of genetic coancestry: Alaska and Canada, central California, continental Santa Barbara channel, Channel Islands (both northern and southern) and the continental southern part of the southern California Bight and Baja California peninsula. Beyond $K = 5$, no additional structure appears (data not shown). Although these clusters are geographically coherent, interesting patterns emerged. Both the northern and southern Channel Islands were part of the same cluster despite the large

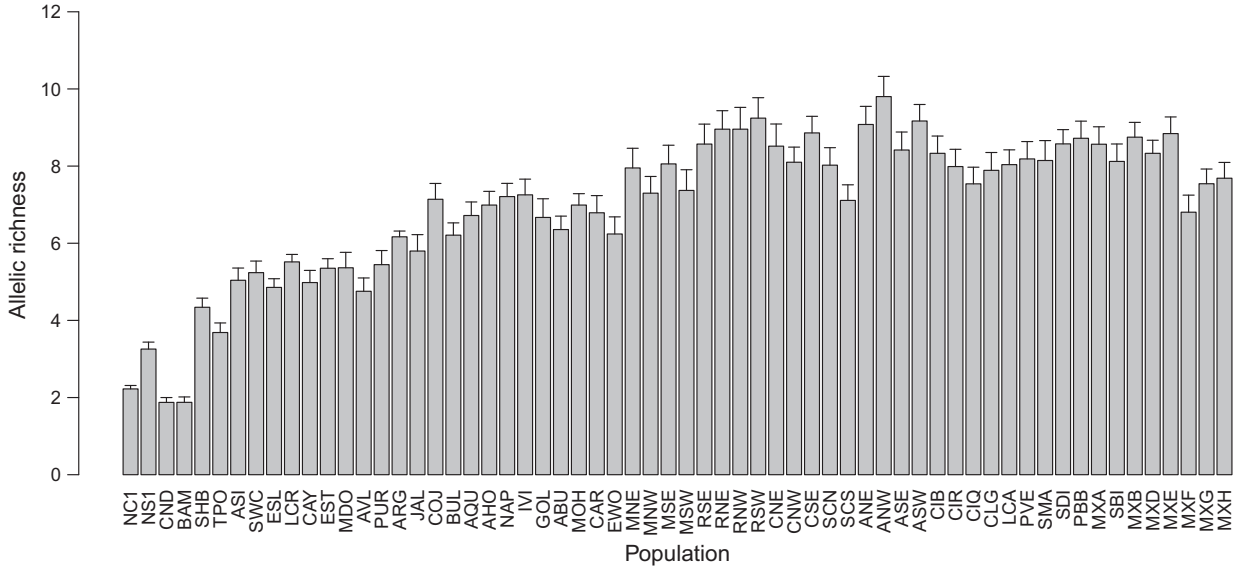

Fig. 2 Allelic richness, standardized to $n = 15$ individuals per sample, in sampled populations of *Macrocystis pyrifera*. Population order from left to right corresponds approximately with their north to south position along the coast. Abbreviations in Table 1.

© 2015 John Wiley & Sons Ltd

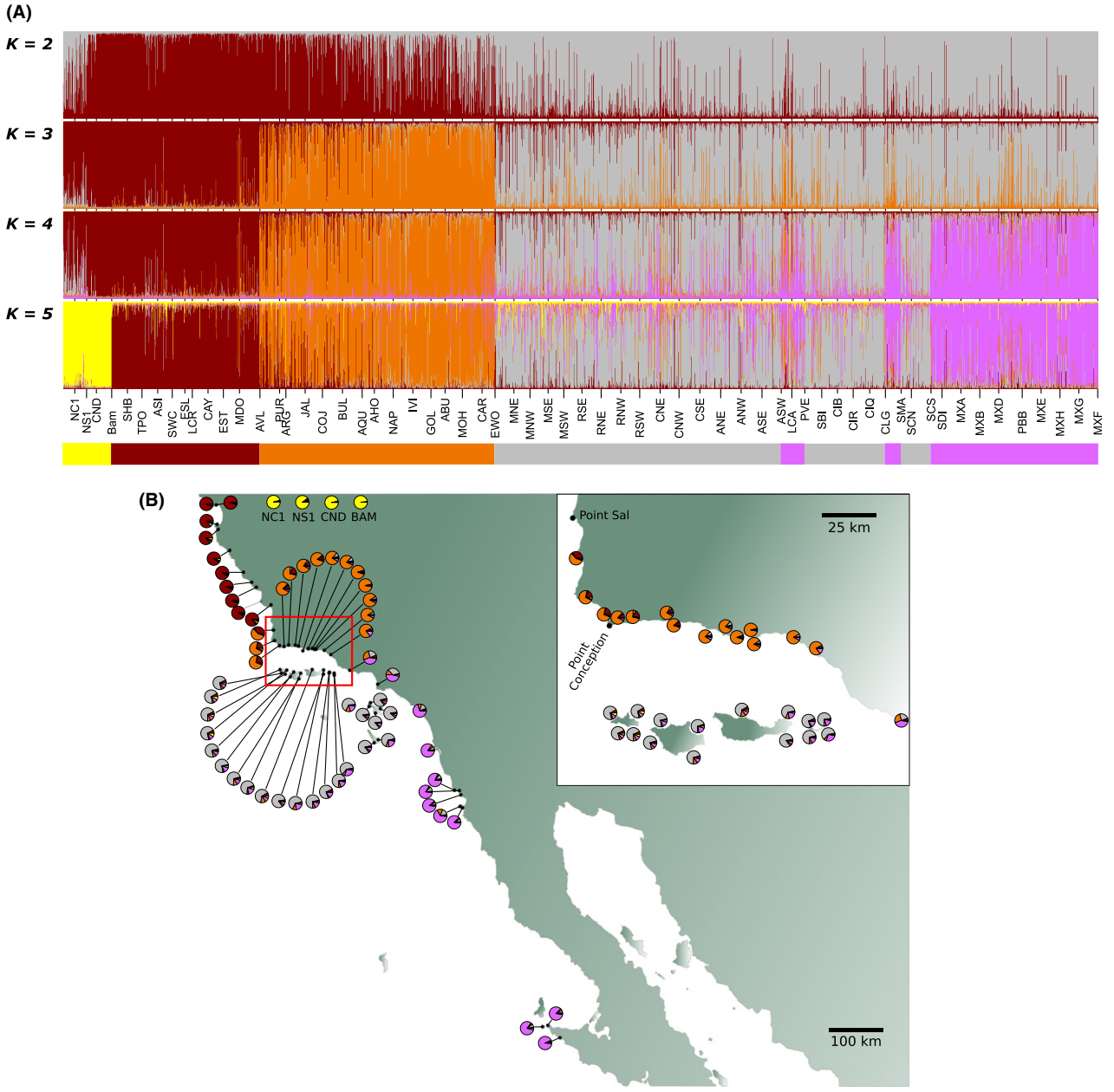

Fig. 3 (Panel A) STRUCTURE bar plots for $K = 2$ to $K = 5$. Population order from left to right corresponds approximately with their north to south position along the coast. Full population names and locations are listed in Table 1. Vertical bar colours represent cluster memberships in each row. $K = 5$ cluster memberships for populations are indicated by the bar colours below population names: Canada/Alaska (yellow), central California (red), Santa Barbara mainland (orange), Channel Islands (grey), southern California/Baja California peninsula (orchid). (Panel B) Distribution of $K = 5$ STRUCTURE clusters for *Macrocystis pyrifera* in the northeast Pacific. Data are presented as the mean individual membership coefficient (proportion of an individual's genome inherited from ancestors in a particular population) for a given sampling location. Northern populations (Canada and Alaska) are shown across the land at the top of the figure. $K = 5$ cluster memberships for populations are indicated by the pie chart colours: Canada/Alaska (yellow), central California (red), Santa Barbara mainland (orange), Channel Islands (grey), southern California/Baja California peninsula (orchid).

extent of open ocean between these systems, and this group excluded the much closer continental populations in both the north and south. The southernmost mainland cluster also extended for around 1000 km of coastline and across an area with low habitat continuity along the Baja California peninsula.

The genetic distance network best matching our STRUCTURE classification resulted from pruning edges until

© 2015 John Wiley & Sons Ltd

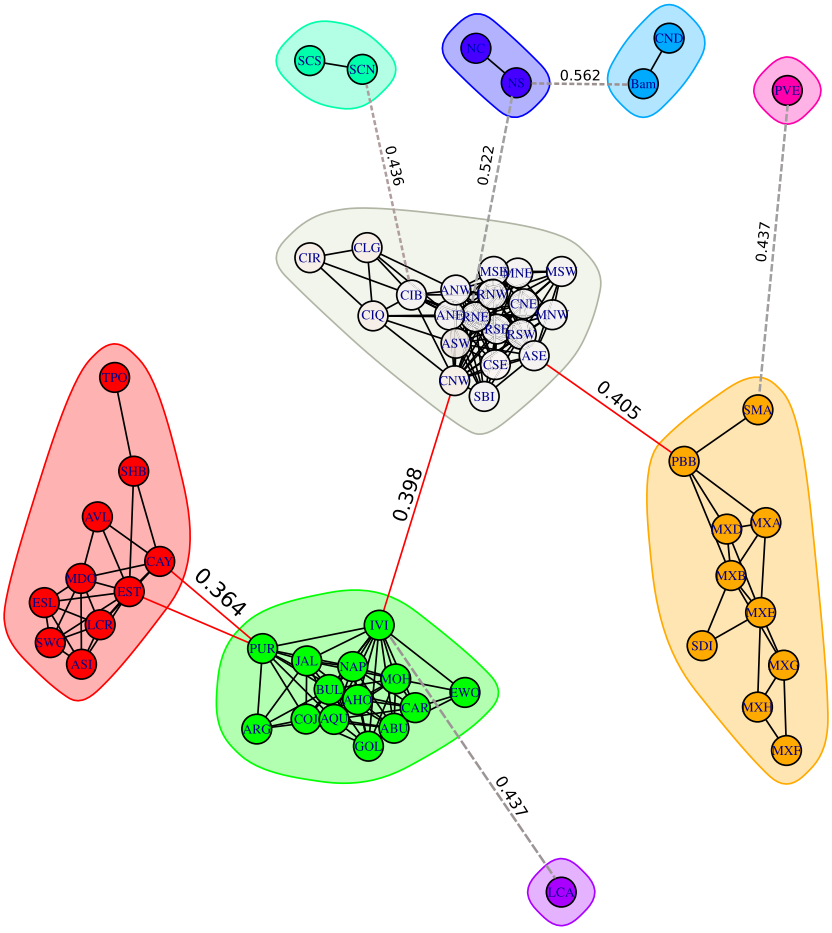

Fig. 4 Network of *Macrocystis* microsatellite genetic differentiation (Cavalli-Sforza and Edwards chord distances). The topology results from pruning the network for pairwise genetic distances smaller or equal than 0.41. Network communities are represented by different colours and were characterized using a community detection algorithm (see Materials and methods). Edges within communities are represented by solid lines in black and edges between communities by red lines. Communities retained in the larger network are central California (red), Santa Barbara channel (green), northern Channel Islands plus Catalina Island (white) and southern and Baja California (yellow). The smallest chord distance value between two communities is shown. Smaller distances are printed with larger font size to represent higher genetic similarity. Population classification to network communities is in agreement with that of STRUCTURE clusters (Fig. 3). The clusters that separated from the network before the threshold value of 0.41 was reached are shown linked by a broken grey edge and the threshold value at the break shown.

six unconnected subnetworks were produced. Subnetworks consisted of the two Alaska populations together, the two Canada populations together, the two San Clemente Island populations in one subnetwork, Palos Verdes alone, Leo Carrillo alone and the remaining populations grouped in a single large subnetwork (Fig. 4). Within this large subnetwork, the population classification into network communities largely confirmed the $K = 5$ classification obtained with STRUCTURE. However, this analysis is not redundant because the network allows visualizing putative patterns of genetic connectivity. Most interestingly, connections in the network follow expectations based on geography: central California (red) is connected to Purisma, the northernmost Santa Barbara channel group site (green), while the Channel Islands' community (white) is positioned at the intersection of two mainland communities, on the network path between the Santa Barbara channel group (green) and the remaining southern populations (yellow).

Based on adjusted Rand distance, the best match between network communities identified from different seasonal minimum mean oceanographic transport time networks and STRUCTURE clusters was obtained for the summer network, with one cluster and three communities (Fig. S1, Supporting information). The summer ocean transport network community analysis recovered the southern California Mainland STRUCTURE cluster perfectly (Fig. S1, Supporting information). However, community analysis disagreed with STRUCTURE regarding the affinity of the northern Channel Islands. Community analysis identified a single group consisting of ROMS cells from the Santa Barbara Mainland and the northern Channel Islands, whereas STRUCTURE genetic analysis grouped all the Channel Islands into a single cluster, separate from the Santa Barbara Mainland. This analysis demonstrates that oceanographic transport alone, as represented here, cannot explain all the genetic patterns, specifically why all Channel Islands belong to the same genetic cluster.

To explore possible isolation-by-environment associations that could also shed light on the partial disconnect between oceanographic connectivity and genetic structure, we used CCA to quantify the associations between environmental predictors and a STRUCTURE clustering model based on $K = 4$ (i.e. excluding Canada and Alaska populations). Stepwise model selection in the

© 2015 John Wiley & Sons Ltd

CCA analysis (Fig. 5) identified PAR, light extinction coefficient, sea surface temperature, latitude and longitude as significant predictors associated with STRUCTURE coancestry clusters. Variance partitioning showed that 64% of the total variance could be explained by our environmental predictors and latitude and longitude. Of this explainable variance, 33% was explained by latitude and longitude, 52% by environment and 15% of the variance was jointly explained. The CCA plot in Fig. 5 shows that latitude and longitude axes align almost perfectly, which is likely due to the sampling domain following a northeast–southwest direction. As expected, sites are generally well positioned according to their sampling coordinates along this geographical axis and close to the genetic response cluster to which they belong (*K* codes shown in the plot). Both PAR and sea surface temperature predictors have axes that are nearly parallel with the geographical axes. This is evidence of spatial autocorrelation between environment and geography, resulting in confounded effects in their association with the genetic classification. However, the light extinction coefficient predictor had a CCA axis perpendicular to the geographical axis and aligned with the Channel Islands cluster (*K*3) ordination in the CCA plot. Lower levels of light extinction coefficient are associated with the Island habitat where giant kelp is known to colonize deeper (North 1994).

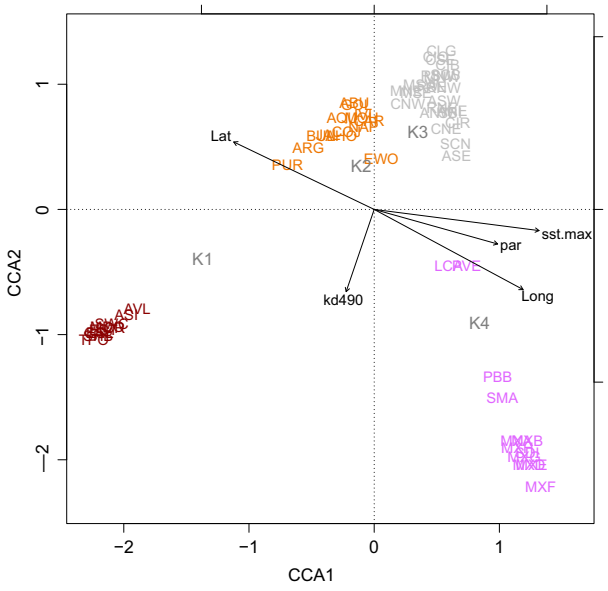

Fig. 5 Canonical correspondence analysis of the association of STRUCTURE cluster assignments in *Macrocystis pyrifera* with maximum summer sea surface temperature (sst.max), light extinction coefficient (kd490), photosynthetically active radiation (par), latitude and longitude. Structure groups are central California (dark red), Santa Barbara (orange), Channel Islands (grey) and southern and Baja California (orchid).

Within-cluster genetic differentiation

The optimized multiple regression model for genetic differentiation in central California retained habitat continuity and transport time (Adj. $R^2 = 0.288$) and had a higher fit than geographic distance (Adj. $R^2 = 0.031$), habitat continuity (Adj. $R^2 = 0.182$) or transport time (Adj. $R^2 = 0.106$) alone (Table 2, Fig. S2, Supporting information). Six pairwise comparisons between populations north and immediately south of Monterey Bay (Fig. S2, circled, Supporting information) appeared to have anomalously high pairwise F_{ST} values. Therefore, we also performed the central California linear regression analysis without the two populations north of Monterey Bay. In this case, geographic distance alone was the best predictor of genetic distance (Adj. $R^2 = 0.431$) when compared to habitat continuity (Adj. $R^2 = 0.058$) or oceanographic transport (Adj. $R^2 = 0.376$). However, oceanographic transport and geographic distance are highly correlated (Pearson's correlation = 0.923), and the difference in variance explained is relatively small.

For the Santa Barbara STRUCTURE cluster, the best-fitting linear model included summer sea surface temperature difference and January minimum transport time (Table 2, Fig. S3, Supporting information, Adj. $R^2 = 0.798$). Results for distance alone (Adj. $R^2 = 0.710$) and January minimum transport time alone (Adj. $R^2 = 0.746$) were also highly significant, but were a worse fit to the data. Habitat continuity (Adj. $R^2 = -0.011$) was a poor fit to the data.

For the STRUCTURE cluster incorporating all of the southern California Bight south of the Santa Barbara Channel, the best predictor of genetic distance was summer minimum transport time (Table 2, Fig. S4, Supporting information, Adj. $R^2 = 0.625$). Simple linear regressions for distance (Adj. $R^2 = 0.417$) and habitat continuity (Adj. $R^2 = 0.148$) were both significant, but explained less variance than summer minimum transport time.

Discussion

Our biogeographical scale analysis showed that *Macrocystis* in the northeast Pacific can be divided genetically into five main geographic clusters: Alaska/Canada, central California, continental Santa Barbara Channel, Channel Islands and the southern part of the southern California Bight/Baja California peninsula. The STRUCTURE hierarchical analysis indicates that the strongest genetic break in the study area divides a northern (all of central California) from a southern (Channel Islands and mainland populations south from the Emma Wood

© 2015 John Wiley & Sons Ltd

Table 2 Single- and multiple-term models used to predict genetic differentiation ($F_{ST}/1 - F_{ST}$) in *Macrocystis pyrifera*

Model	Partial regression slopes	Standard partial regression slopes	BIC	Adj. R^2	*P* value
Central California					
$F_{ST}/1 - F_{ST}$ ~ Habitat Continuity +	-5.09×10^{-1}	4.42×10^{-1}	−95.41	0.288	4.22×10^{-3}
Transport Time	2.82×10^{-3}	3.47×10^{-1}			
IBD Model			−84.87	0.031	0.13
Habitat Continuity			−92.16	0.182	2.51×10^{-3}
Oceanographic Transport (5 km Model)			−88.31	0.106	0.02
Central California (Minus TPO/SHB)					
$F_{ST}/1 - F_{ST}$ ~ Distance			−84.17	0.431	1.20×10^{-4}
Habitat Continuity			−70.56	0.058	0.12
Oceanographic Transport (5 km Model)			−81.68	0.376	4.00×10^{-4}
Santa Barbara Channel					
$F_{ST}/1 - F_{ST}$ ~ Summer SST Difference +	1.22×10^{-2}	2.72×10^{-1}	−430.78	0.798	$<2.2 \times 10^{-16}$
January Min Transport Time	5.13×10^{-3}	7.24×10^{-1}			
IBD Model			−401.12	0.71	$<2.2 \times 10^{-16}$
Habitat Continuity			−287.53	−0.011	0.98
Oceanographic Transport (January Minimum)			−413.27	0.746	$<2.2 \times 10^{-16}$
Southern California					
$F_{ST}/1 - F_{ST}$ ~ Summer Minimum Transport Time			−1556.78	0.625	$<2.2 \times 10^{-16}$
IBD Model			−1426.16	0.417	$<2.2 \times 10^{-16}$
Habitat Continuity			−1313.25	0.148	4.00×10^{-12}

For multiple-term models, partial regression slopes and standardized partial regression slopes are indicated. For all models, the Bayesian model selection criteria (BIC) and the adjusted coefficient of determination (Adj. R^2) are shown. Overall significance of regression models is indicated with *F*-test *P* values.
IBD, Isolation by distance; TPO/SHB, Terrace Point and Sandhill Bluff (populations north of Monterey Bay); SST, sea surface temperature.

sampling site, including the Baja California peninsula) group. The Santa Barbara mainland sites, between the northern and southern groups, display a genetic signature consistent with a transition zone and form a distinct genetic cluster. Thus, the strongest phylogeographic barrier in giant kelp in the northeast Pacific is associated with two well-known biogeographic transition regions flanking the mainland Santa Barbara channel region: in the south, the narrow seaway between Point Hueneme and the northern Channel Islands, and in the north, the area around Point Conception.

Current patterns and bathymetry likely interact to limit exchange of propagules between mainland Santa Barbara and mainland southern California/Baja California peninsula populations. The narrow seaway between Point Hueneme and the northern Channel Islands probably limits the transport of propagules northward into the Santa Barbara Channel (Dawson 2001), while cyclonic gyre circulation in the Santa Barbara Channel and southern California Bight may limit transport between the two regions (Hickey 1992; Dong *et al.* 2009). Support for this hypothesis is provided by Mitarai *et al.* (2009) who demonstrated that ROMS simulated particles released within the Santa Barbara Channel tended to remain in the Channel, while particles released in the southern Channel Islands tended to remain in the southeastern part of the Bight. This break is best explained as the result of interacting currents and the relatively short duration of the competency period of giant kelp spores (Reed *et al.* 1992; Mitarai *et al.* 2009) resulting in the loss of many spores in deep water or areas of inappropriate substrate between habitat patches.

It has been hypothesized that the predominance of southward-flowing currents along the California coast may play a significant role in limiting dispersal of larvae

© 2015 John Wiley & Sons Ltd

and spores north of Point Conception (Roy *et al.* 1995; Wares *et al.* 2001). Eberl *et al.* (2013) identified a significant genetic break at the Point Conception biogeographic boundary in the supralittoral isopod *Ligia occidentalis*, and a review by Pelc *et al.* (2009) found marginally significant clustering of phylogeographical breaks in planktonic dispersing species at Point Conception. However, our STRUCTURE results failed to find a break at Point Conception. Instead, we identified the break as occurring near Point Sal, ~50 km north of Point Conception. This break is consistent with a simulation study by Hohenlohe (2004) using a gene flow model that included the observed temporal variation in ocean currents in this area (75–90% southward-flowing, 10–25% northward-flowing currents, Harms & Winant 1998); incorporating this variation shifted the genetic break northward of Point Conception when compared to a constantly southward-flowing current model. Other research has similarly suggested that transport is not limited by Point Conception. Washburn *et al.* (2011) demonstrated that periodic relaxations of prevailing upwelling-favourable winds could result in the occasional transport of warm waters from within the Santa Barbara Channel poleward around Point Conception and potentially as far as Point Sal. Thus, while some level of genetic differentiation may occur across Point Conception, other breaks elsewhere in California may be equally or more important (Burton 1998; Dawson 2001).

Unexpectedly, the Channel Islands formed a genetic cluster, distinct from the adjacent mainland Santa Barbara sites in the north and mainland sites near Los Angeles in the south. This Channel Islands genetic cluster was not supported by oceanographic transport. While network analysis based on oceanographic transport in southern California recovered the mainland southern California STRUCTURE cluster intact as one community, the analysis united the Santa Barbara coast and northern Channel Islands as a second community and identified the southern Channel Islands as a third. Thus, oceanographic transport alone does not explain all the genetic classification estimated in STRUCTURE. The environmental network most closely matching our STRUCTURE clusters was one with edges representing habitat continuity between populations (analysis not shown). However, this analysis also failed to join together the northern and southern Channel Islands, as expected given the large body of deep water between them.

The northern and southern Channel Islands were genetically similar despite low oceanographic connectivity between them, while each was genetically distinct from their neighbouring mainland sites. We note that the oceanographic connectivity network analysis supports the differentiation between southern Channel Islands and mainland, but the dissimilarity between northern Channel Islands and the Santa Barbara mainland cannot be similarly explained. This result is consistent with isolation by environment (Wang & Bradburd 2014) because with neutral markers such as microsatellites, some level of gene flow is needed to balance the effects of genetic drift for low genetic differentiation to be maintained between disjunct regions, even if both are under similar selection pressure. Connectivity between the northern and southern Channel Islands should be extremely limited based on the dispersal capability of *Macrocystis* and patterns of ocean transport as estimated by ROMS. For example, 4–5 days are necessary for a spore to bridge the distance between the two regions even in the spring when transport times are shortest (ROMS data, not shown). By itself, this result is very interesting as an indicator of potential gene flow over long distances of water in giant kelp. On the other hand, spores can transit between the Santa Barbara mainland and the northern Channel Islands during spring in only 2 days (ROMS data, not shown). This suggests that the fitness of the migrants must be different from that of natives in the new environment for dispersal not to homogenize the gene pools across the Santa Barbara Channel, as observed between the northern and southern Channel Islands. Demographic density-barrier effects (competitive advantage of prior colonizers) may also maintain distinct adjacent gene pools despite oceanographic transport, as shown by long-term absence of gene flow across neighbouring populations in other brown algae (Neiva *et al.* 2012a,b).

Consistent with the possibility of an isolation-by-environment scenario, CCA analysis showed that STRUCTURE clusters were associated with sea surface temperature, PAR, light extinction coefficient, latitude and longitude. As both sea surface temperature and PAR are strongly correlated with latitude and longitude, these associations are confounded with geographic distance and thus challenging to interpret. Light extinction coefficient (kd490 in Fig. 5), however, was not correlated with latitude and longitude, but showed a strong association with the Channel Island populations.

The greater light penetration in the Channel Islands is accompanied by other ecological differences that may impact survival of immigrant spores there. It is also correlated with a larger than presently apparent past continuity, as there is more extensive favourable habitat due to light penetration and this effect was even larger in the past periods when sea level was lower. Other environmental effects have been suggested to influence island/continent differences in *Macrocystis*, such as by Kopczak *et al.* (1991) who demonstrated that in the lower nitrate levels of Catalina Island, *Macrocystis* were more efficient at assimilating nitrate than those from mainland Santa Barbara or central California although

© 2015 John Wiley & Sons Ltd

such differences might be acclimation rather than adaptation. Given the highly competitive environment of the kelp forest (Johansson *et al.* 2013), even small differences in nutrient uptake or competitive ability could doom immigrants to failure in the islands, although competitive exclusion may also simply be maintained by demographic prior-colonization density-barrier effects, without the need to invoke adaptive differences (Neiva *et al.* 2012a,b). In transplant experiments performed on Catalina Island, Kopczak *et al.* (1991) found that although survivorship among hundreds of transplanted juvenile sporophytes from Santa Barbara, Monterey, or Catalina Island was generally very low, only individuals from Catalina survived longer than 2 weeks, with six of these individuals surviving to reproductive maturity.

The unexpectedly high connectivity seen in the Channel Islands genetic cluster is somewhat replicated in the southern California mainland/Baja California peninsula cluster, which encompasses a large coastal stretch, extending from north of Los Angeles to the southern limit of distribution in the Northern hemisphere in Baja California Sur. This large spatial extent encompasses a stretch of coastline along Bahia Sebastian Vizcaino in the central Baja California peninsula where *Macrocystis* is absent for approximately 300 km due to a lack of appropriate substrate. The high allelic diversity observed here, which is near maximum except for the last two sites close to the distribution limit, is consistent with the classical view of southern refuge during the last glacial maximum in the Northern hemisphere (Hewitt 2000). However, severe declines in giant kelp abundance caused by the 1997–1998 El Niño Southern Oscillation (ENSO) in this area (Ladah *et al.* 1999) should have reduced allelic diversity and increased genetic differentiation among populations. The absence of such a pattern reveals that giant kelp could maintain a high level of genetic diversity during these periods and supports hypotheses concerning the role of arrested development of microscopic stages during adverse periods (Ladah *et al.* 1999; Carney *et al.* 2013) or refugia in deeper water (Ladah & Zertuche-González 2004).

When we performed linear regression analysis within each STRUCTURE group, we found a clear relationship between genetic differentiation and oceanographic transport. This is consistent with our previous results along the Santa Barbara coast (Alberto *et al.* 2011). In central California, the best-fitting model incorporated habitat continuity and transport time as explanatory variables. When the two northernmost populations were removed (to eliminate pairwise comparisons spanning Monterey Bay), a single-term isolation-by-distance model became the best fit, although the single-term model with oceanographic transport as the predictor was also significant and explained only 6% less variation in genetic distance. These variables were highly correlated (Pearson 0.92), and this small difference can thus be caused by slight variation in F_{ST} estimates, distance measures or transport model results.

Along the mainland coast near Santa Barbara, the best-fit model incorporated summer sea surface temperature difference and January minimum transport time, contrary to a previous study of the Santa Barbara mainland, where June minimum transport was the best predictor of genetic STRUCTURE (Alberto *et al.* 2011). Because Pearson's correlations between all of our monthly minimum transport times are high (>0.74), it is conceivable that the difference between the two analyses may result from slight variations in parameter estimates. However, when we trimmed the Santa Barbara data set to include only the eight populations examined by Alberto *et al.* (2011), the best fit model was a two-predictor model with June minimum transport time and summer sea surface temperature difference (data not shown, Adj. $R^2 = 0.87$, $P = 5.2 \times 10^{-12}$). The consistency of this result with that of Alberto *et al.* (2011) is robust because different kelp samples were used for the two studies and argues for the importance of strong currents in explaining the patterns of genetic diversity in *Macrocystis*. Consistent with this notion is our finding that minimum transport time in the summer was the single best predictor of genetic differentiation in *Macrocystis* for the entire southern California region.

June is the month with the shortest transport times and the greatest westward asymmetry and coincides with the highest level of spore production and release along the Santa Barbara coast (Reed *et al.* 1996; Alberto *et al.* 2011). Maximizing spore release during times of strong currents and short interpopulation transport times would tend to promote gene flow between populations. Finding that January transport time explains more variation in pairwise genetic differentiation when all 14 Santa Barbara cluster populations are considered probably reflects intra-annual variation in conditions that promote sporophyte recruitment (Reed 1990; Reed *et al.* 1997), as well as the dynamic nature of currents in the Santa Barbara region. During the summer, the transport of spores to populations northwest of Point Conception is limited by the southward-flowing California Current, and by cyclonic gyre circulation in the Santa Barbara Channel (Mitarai *et al.* 2009). In addition, strong currents and strong upwelling in the vicinity of Point Conception may promote advection of spores offshore and prevent spore settlement (Dong & McWilliams 2007; White *et al.* 2010). Poleward water movements associated with deep-lying countercurrents (Drake *et al.* 2011) and relaxations of upwelling-favourable winds (Washburn *et al.* 2011) may occasionally transport

© 2015 John Wiley & Sons Ltd

propagules northward across Point Conception in spring and summer, when prevailing currents are southward. However, more pronounced relaxations and reversals of the Santa Barbara Channel eddy and California Current in winter (Dong & McWilliams 2007; Mitarai *et al.* 2009) may account for why minimum transport times in January best explain the genetic structure along the broader mainland coast of Santa Barbara. Temporal variability in nearshore surface currents has been demonstrated to affect metapopulation connectivity in species pairs with differing reproductive timing (Carson *et al.* 2010). By producing spores throughout the year, as it does in some California areas (Reed *et al.* 1996), *Macrocystis* may be able to bypass seasonal reproductive barriers associated with these variable currents (Hohenlohe 2004).

Linear models for two subsets of the data also identified a significant role for habitat characteristics in structuring gene flow in *Macrocystis*: central California (habitat continuity), and Santa Barbara mainland (summer sea surface temperature). Habitat continuity was associated with genetic differentiation in giant kelp along the Santa Barbara coast (Alberto *et al.* 2010, 2011), but not in the current study, either among the complete set of Santa Barbara coast populations or the subset of populations examined in the previous studies. We found a significant association between habitat continuity and genetic differentiation in central California, where Monterey Bay represents a relatively large patch of sandy habitat along a coastline largely characterized by stretches of rocky substrate (Dawson 2001). When we eliminated comparisons across Monterey Bay, the relationship between habitat and genetic distance disappeared, suggesting that this habitat gap may have produced the pattern. Our failure to find a relationship between habitat and genetic structure in the southern California Bight contrasts with results from three species examined by Selkoe *et al.* (2010), where kelp cover correlated strongly with genetic patterns. Sea surface temperature and genetic differentiation showed a significant linear relationship along the Santa Barbara coast. This area falls within the region of greatest interaction between the cold, southward-flowing California Current and the warm, northward-flowing waters from southern California. In spite of the relationship between oceanography, distance and temperature in the area, our analysis suggests that sea surface temperature has effects above and beyond its correlation with distance alone.

Conclusions

This study demonstrates the power of conducting a hierarchical analysis when analysing large extents of a species distribution to extricate the nested structure and processes that shape genetic differentiation at different spatial and temporal scales. At the largest scale, oceanographic transport models are not sufficient to consistently explain the observed genetic coancestry clusters. Patterns of isolation by environment in giant kelp between the Channel Islands and mainland giant kelp forests should be further investigated experimentally to test hypotheses concerning adaptation to different environments (Nosil *et al.* 2008). Within the genetic clusters, we showed that previous findings on the important role played by oceanographic transport in giant kelp's genetic connectivity (Alberto *et al.* 2011) generalize well to other areas of its distribution.

Acknowledgements

The authors would like to thank E. Latch for assistance with STRUCTURE analysis, H. Hargarten for helpful comments and discussion on earlier drafts of the manuscript, D. Siercks for assistance with parallel computing, J. Nicholls for advice on graph preparation and L. Carney, S. Harrer, C. Nelson and C. Donahue for help collecting samples. Comments from two anonymous reviewers greatly improved the final manuscript. Financial support for this research was provided by Portuguese Science Foundation FCT grants MEGIKELP PTDC/MAR/65461/2006, cofunded by FEDER and EXCL/AAG-GLO/0661/2012, by a grant from the U.S. National Science Foundation's Long Term Ecological Research Program to the Santa Barbara Channel LTER and by NSF OCE Biological Oceanography Program grants to D. Reed, P. Raimondi and F. Alberto (OCE-1233839), and P. Drake and C. Edwards (OCE-1260693). The ICE team assisted with the Baja California peninsula collections, funded by SEP-CONACYT and UC MEXUS-CONACYT grants to LBL.

References

Alberto F (2009) MsatAllele_1.0: An R package to visualize the binning of microsatellite alleles. *The Journal of Heredity*, **100**, 394–397.

Alberto F, Arnaud-Haond S, Duarte C, Serrão E (2006) Genetic diversity of a clonal angiosperm near its range limit: the case of *Cymodocea nodosa* at the Canary Islands. *Marine Ecology Progress Series*, **309**, 117–129.

Alberto F, Whitmer A, Coelho NC *et al.* (2009) Microsatellite markers for the giant kelp *Macrocystis pyrifera*. *Conservation Genetics*, **10**, 1915–1917.

Alberto F, Raimondi PT, Reed DC *et al.* (2010) Habitat continuity and geographic distance predict population genetic differentiation in giant kelp. *Ecology*, **91**, 49–56.

Alberto F, Raimondi PT, Reed DC *et al.* (2011) Isolation by oceanographic distance explains genetic structure for *Macrocystis pyrifera* in the Santa Barbara Channel. *Molecular Ecology*, **20**, 2543–2554.

Amaral AR, Beheregaray LB, Bilgmann K *et al.* (2012) Seascape genetics of a globally distributed, highly mobile marine mammal: the short-beaked common dolphin (genus *Delphinus*). *PLoS One*, **7**, e31482.

© 2015 John Wiley & Sons Ltd

Assis J, Serrão EA, Claro B, Perrin C, Pearson GA (2014) Climate-driven range shifts explain the distribution of extant gene pools and predict future loss of unique lineages in a marine brown alga. *Molecular Ecology*, **23**, 2797–2810.

Assis J, Zupan M, Nicastro KR, Zardi GI, McQuaid CD, Serrão EA (2015) Oceanographic Conditions Limit the Spread of a Marine Invader along Southern African Shores. *PLoS One*, **10**, e0128124.

Avise J (1992) Molecular population structure and the biogeographic history of a regional fauna: a case history with lessons for conservation biology. *Oikos*, **63**, 62–76.

Avise JC (2004) *Molecular Markers, Natural History, and Evolution*. Sinauer Associates Inc, Sunderland, Massachusetts.

Balkenhol N, Waits LP, Dezzani RJ (2009) Statistical approaches in landscape genetics: an evaluation of methods for linking landscape and genetic data. *Ecography*, **32**, 818–830.

Belanger CL, Jablonski D, Roy K, Berke SK, Krug AZ, Valentine JW (2012) Global environmental predictors of benthic marine biogeographic structure. *Proceedings of the National Academy of Sciences of the United States of America*, **109**, 14046–14051.

Belkhir K, Borsa P, Chikhi L, Raufaste N, Bonhomme F (2004) *GENETIX 4.05, logiciel sous Windows TM pour la génétique des populations*. Laboratoire Génome, Populations, Interactions, CNRS UMR 5171, Université de Montpellier II, Montpellier (France). Available at http://kimura.univ-montp2.fr/genetix/.

Bell TW, Cavanaugh KC, Reed DC, Siegel DA (2015) Geographical variability in the controls of giant kelp biomass dynamics. *Journal of Biogeography*, **42**, 2010–2021.

Blondel VD, Guillaume J-L, Lambiotte R, Lefebvre E (2008) Fast unfolding of communities in large networks. *Journal of Statistical Mechanics*, P10008.

Bohonak AJ (1999) Dispersal, gene flow, and population structure. *The Quarterly Review of Biology*, **74**, 21–45.

Boland W, Marner F, Jaenicke L, Muller D, Folster E (1983) Comparative receptor study in gamete chemotaxis of the seaweeds *Ectocarpus siliculosus* and *Cutleria multifida*. *European Journal of Biochemistry*, **134**, 97–103.

Borcard D, Legendre P, Drapeau P (1992) Partialling out the spatial component of ecological variation. *Ecology*, **73**, 1045–1055.

Briggs JC (1974) *Marine Zoogeography*. McGraw-Hill, New York.

Burton RSR (1998) Intraspecific phylogeography across the Point Conception biogeographical boundary. *Evolution*, **52**, 734–745.

Carney LT, Bohonak AJ, Edwards MS, Alberto F (2013) Genetic and experimental evidence for a mixed-age, mixed-origin bank of kelp microscopic stages in southern California. *Ecology*, **94**, 1955–1965.

Carson HS, López-Duarte PC, Rasmussen L, Wang D, Levin LA (2010) Reproductive timing alters population connectivity in marine metapopulations. *Current Biology*, **20**, 1926–1931.

Castorani MCN, Reed DC, Alberto F *et al.* (in press) Connectivity structures local population dynamics: a long-term empirical test in a large metapopulation system. *Ecology*. doi: 10.1890/15-0283.1.

Cavanaugh KC, Siegel DA, Reed DC, Dennison PE (2011) Environmental controls of giant kelp biomass in the Santa Barbara Channel, California. *Marine Ecology Progress Series*, **429**, 1–17.

Cavanaugh KC, Siegel DA, Raimondi PT, Alberto F (2014) Patch definition in metapopulation analysis: a graph theory approach to solve the mega-patch problem. *Ecology*, **95**, 316–328.

Chapuis M-P, Estoup A (2007) Microsatellite null alleles and estimation of population differentiation. *Molecular Biology and Evolution*, **24**, 621–631.

Clauset A, Newman M, Moore C (2004) Finding community structure in very large networks. *Physical Review E*, **70**, 066111.

Coleman MA, Roughan M, Macdonald HS *et al.* (2011) Variation in the strength of continental boundary currents determines continent-wide connectivity in kelp. *Journal of Ecology*, **99**, 1026–1032.

Coscia I, Robins PE, Porter JS, Malham SK, Ironside JE (2013) Modelled larval dispersal and measured gene flow: seascape genetics of the common cockle *Cerastoderma edule* in the southern Irish Sea. *Conservation Genetics*, **14**, 451–466.

Cowen RK, Sponaugle S (2009) Larval dispersal and marine population connectivity. *Annual Review of Marine Science*, **1**, 443–466.

Coyer JA, Smith GJ, Andersen RA (2001) Patterns of *Macrocystis pyrifera* (Phaeophyceae) evolution and biogeography as determined by ITS1 and ITS2 sequences. *Journal of Phycology*, **37**, 574–585.

Csardi G, Nepusz T (2006) The IGRAPH software package for complex network research. *InterJournal Complex Systems*, **1695**.

D'Aloia CC, Bogdanowicz SM, Harrison RG, Buston PM (2014) Seascape continuity plays an important role in determining patterns of spatial genetic structure in a coral reef fish. *Molecular Ecology*, **23**, 2902–2913.

Dawson M (2001) Phylogeography in coastal marine animals: a solution from California? *Journal of Biogeography*, **28**, 723–736.

Dee DP, Uppala SM, Simmons AJ *et al.* (2011) The ERA-Interim reanalysis: configuration and performance of the data assimilation system. *Quarterly Journal of the Royal Meteorological Society*, **137**, 553–597.

Demes KW, Graham MH, Suskiewicz TS (2009) Phenotypic plasticity reconciles incongruous molecular and morphological taxonomies: the giant kelp, *Macrocystis* (Laminariales, Phaeophyceae), is a monospecific genus. *Journal of Phycology*, **45**, 1266–1269.

Dong C, McWilliams JC (2007) A numerical study of island wakes in the Southern California Bight. *Continental Shelf Research*, **27**, 1233–1248.

Dong C, Idica EY, McWilliams JC (2009) Circulation and multiple-scale variability in the Southern California Bight. *Progress in Oceanography*, **82**, 168–190.

Donlon CJ, Martin M, Stark J, Roberts-Jones J, Fiedler E, Wimmer W (2012) The Operational Sea Surface Temperature and Sea Ice Analysis (OSTIA) system. *Remote Sensing of Environment*, **116**, 140–158.

Doyle R (1985) *Biogeographical Studies of Rocky Shore Near Point Conception*. University of California, Santa Barbara, California.

Drake PT, Edwards CA, Barth JA (2011) Dispersion and connectivity estimates along the U.S. west coast from a realistic numerical model. *Journal of Marine Research*, **69**, 1–37.

Drake PT, Edwards CA, Morgan SG, Dever EP (2013) Influence of larval behavior on transport and population connectivity in a realistic simulation of the California Current System. *Journal of Marine Research*, **71**, 317–350.

Drake PT, Edwards CJ, Morgan SG (in press) The relationship between larval settlement and upwelling-related metrics in a

© 2015 John Wiley & Sons Ltd

numerical model of the central California coastal circulation. *Marine Ecology Progress Series*. doi: 10.3354/meps11393.

Eberl R, Mateos M, Grosberg RK, Santamaria CA, Hurtado LA (2013) Phylogeography of the supralittoral isopod *Ligia occidentalis* around the Point Conception marine biogeographical boundary (ed. Bellwood D). *Journal of Biogeography*, **40**, 2361–2372.

ESRI (2011) *ArcGIS Desktop: Release 10*. Environmental Systems Research Institute, Redlands, California.

Evanno G, Regnaut S, Goudet J (2005) Detecting the number of clusters of individuals using the software STRUCTURE: a simulation study. *Molecular Ecology*, **14**, 2611–2620.

Excoffier L, Lischer HEL (2010) ARLEQUIN suite ver 3.5: a new series of programs to perform population genetics analyses under Linux and Windows. *Molecular Ecology Resources*, **10**, 564–567.

Foster MSM, Schiel DDR (1985) The ecology of giant kelp forests in California: a community profile. *US Fish & Wildlife Service Biological Report*, **85**, 1–152.

Galindo HM, Olson DB, Palumbi SR (2006) Seascape genetics: a coupled oceanographic-genetic model predicts population structure of Caribbean corals. *Current Biology*, **16**, 1622–1626.

Gaylord B, Reed DC, Raimondi PT, Washburn L, McLean SR (2002) A physically based model of macroalgal spore dispersal in the wave and current-dominated nearshore. *Ecology*, **83**, 1239–1251.

Gilg M, Hilbish T (2003) The geography of marine larval dispersal: coupling genetics with fine-scale physical oceanography. *Ecology*, **84**, 2989–2998.

Gonzalez I, Dejean S, Martin PGP, Baccini A (2008) CCA: An R package to extend canonical correlation analysis. *Journal of Statistical Software*, **23**, 1–14.

Graham MH, Vasquez JA, Buschmann AH (2007) Global ecology of the giant kelp Macrocystis: from ecotypes to ecosystems. *Oceanography and Marine Biology*, **45**, 39–88.

Hardy OJ, Vekemans X (1999) Isolation by distance in a continuous population: reconciliation between spatial autocorrelation analysis and population genetics models. *Heredity*, **83**, 145–154.

Harms S, Winant CD (1998) Characteristic patterns of the circulation in the Santa Barbara Channel. *Journal of Geophysical Research: Oceans*, **103**, 3041–3065.

Hernández-Carmona G, Hughes B, Graham MH (2006) Reproductive longevity of drifting kelp *Macrocystis pyrifera* (Phaeophyceae) in Monterey Bay, USA. *Journal of Phycology*, **42**, 1199–1207.

Hewitt G (2000) The genetic legacy of the Quaternary ice ages. *Nature*, **405**, 907–913.

Hickey B (1992) Circulation over the Santa Monica-San Pedro basin and shelf. *Progress in Oceanography*, **30**, 37–115.

Hobday A (2000) Abundance and dispersal of drifting kelp *Macrocystis pyrifera* rafts in the Southern California Bight. *Marine Ecology Progress Series*, **195**, 101–116.

Hohenlohe PA (2004) Limits to gene flow in marine animals with planktonic larvae: models of *Littorina* species around Point Conception, California. *Biological Journal of the Linnean Society*, **82**, 169–187.

Holderegger R, Wagner HH (2008) Landscape genetics. *BioScience*, **58**, 199.

Hubert L, Arabie P (1985) Comparing partitions. *Journal of Classification*, **2**, 193–218.

Hutchison DW, Templeton AR (1999) Correlation of pairwise genetic and geographic distance measures: inferring the relative influences of gene flow and drift on the distribution of genetic variability. *Evolution*, **53**, 1898–1914.

Hyde JR, Kimbrell CA, Budrick JE, Lynn EA, Vetter RD (2008) Cryptic speciation in the vermilion rockfish (*Sebastes miniatus*) and the role of bathymetry in the speciation process. *Molecular Ecology*, **17**, 1122–1136.

Johansson ML, Banks MA, Glunt KD, Hassel-Finnegan HM, Buonaccorsi VP (2008) Influence of habitat discontinuity, geographical distance, and oceanography on fine-scale population genetic structure of copper rockfish (*Sebastes caurinus*). *Molecular Ecology*, **17**, 3051–3061.

Johansson ML, Raimondi PT, Reed DC, Coelho NC, Serrão EA, Alberto FA (2013) Looking into the black box: simulating the role of self-fertilization and mortality in the genetic structure of *Macrocystis pyrifera*. *Molecular Ecology*, **22**, 4842–4854.

Jørgensen HBH, Hansen MM, Bekkevold D, Ruzzante DE, Loeschcke V (2005) Marine landscapes and population genetic structure of herring (*Clupea harengus* L.) in the Baltic Sea. *Molecular Ecology*, **14**, 3219–3234.

Keller D, Holderegger R, Van Strien MJ (2013) Spatial scale affects landscape genetic analysis of a wetland grasshopper. *Molecular Ecology*, **22**, 2467–2482.

Kopczak CD, Zimmerman RC, Kremer JN (1991) Variation in nitrogen physiology and growth among geographically isolated populations of the giant kelp, *Macrocystis pyrifera* (Phaeophyta). *Journal of Phycology*, **27**, 149–158.

Ladah LB, Zertuche-González JA (2004) Giant kelp (*Macrocystis pyrifera*) survival in deep water (25–40 m) during El Niño of 1997–1998 in Baja California, Mexico. *Botanica Marina*, **47**, 367–372.

Ladah LB, Zertuche-González JA, Hernández-Carmona G (1999) Giant kelp (*Macrocystis pyrifera*, Phaeophyceae) recruitment near its southern limit in Baja California after mass disappearance during Enso. *Journal of Applied Phycology*, **35**, 1106–1112.

Locke M, Baack E, Toonen R (2000) *Strand* (version 2.2.30). Technical Report, Veterinary Genetics Lab. University of California, Davis, California.

López-Duarte PC, Carson HS, Cook GS *et al.* (2012) What controls connectivity? An empirical, multi-species approach. *Integrative and Comparative Biology*, **52**, 511–524.

Luikart G, England PR, Tallmon D, Jordan S, Taberlet P (2003) The power and promise of population genomics: from genotyping to genome typing. *Nature Reviews Genetics*, **4**, 981–994.

Macaya EC, Zuccarello GC (2010a) DNA Barcoding and genetic divergence in the giant kelp *Macrocystis* (Laminariales). *Journal of Phycology*, **46**, 736–742.

Macaya EC, Zuccarello GC (2010b) Genetic structure of the giant kelp *Macrocystis pyrifera* along the southeastern Pacific. *Marine Ecology Progress Series*, **420**, 103–112.

Maggs CA, Castilho R, Foltz D *et al.* (2008) Evaluating signatures of glacial refugia for north atlantic benthic marine taxa. *Ecology*, **89**, S108–S122.

Martin MJ, Hines A, Bell MJ (2007) Data assimilation in the FOAM operational short-range ocean forecasting system: a description of the scheme and its impact. *Quarterly Journal of the Royal Meteorological Society*, **133**, 981–995.

Martin M, Dash P, Ignatov A *et al.* (2012) Group for High Resolution Sea Surface temperature (GHRSST) analysis fields inter-comparisons. Part 1: a GHRSST multi-product ensemble

© 2015 John Wiley & Sons Ltd

(GMPE). *Deep-Sea Research Part II: Topical Studies in Oceanography*, **77–80**, 21–30.

Mitarai S, Siegel DA, Watson JR, Dong C, McWilliams JC (2009) Quantifying connectivity in the coastal ocean with application to the Southern California Bight. *Journal of Geophysical Research*, **114**, C10026.

Neiva J, Pearson GA, Valero M, Serrão EA (2012a) Fine-scale genetic breaks driven by historical range dynamics and ongoing density-barrier effects in the estuarine seaweed *Fucus ceranoides* L. *BMC Evolutionary Biology*, **12**, 78.

Neiva J, Pearson GA, Valero M, Serrão EA (2012b) Drifting fronds and drifting alleles: range dynamics, local dispersal and habitat isolation shape the population structure of the estuarine seaweed Fucus ceranoides. *Journal of Biogeography*, **39**, 1167–1178.

Neiva J, Assis J, Fernandes F, Pearson GA, Serrão EA (2014) Species distribution models and mitochondrial DNA phylogeography suggest an extensive biogeographical shift in the high-intertidal seaweed *Pelvetia canaliculata*. *Journal of Biogeography*, **41**, 1137–1148.

Newman W (1979) Californian transition zone: significance of short-range endemics. In: *Historical Biogeography, Plate Tectonics, and the Changing Environment* (eds Gray J, Boucot A), pp. 399–416. Oregon State University Press, Corvallis, Oregon.

North W (1994) Review of *Macrocystis* biology. In: *Biology of Economic Algae* (ed. Akatsuka I), pp. 447–527. Academic Publishing, The Hague.

Nosil P, Egan SP, Funk DJ (2008) Heterogeneous genomic differentiation between walking-stick ecotypes: "Isolation by adaptation" and multiple roles for divergent selection. *Evolution*, **62**, 316–336.

Økland RH, Eilertsen O (1994) Canonical correspondence analysis with variation partitioning: some comments and an application. *Journal of Vegetation Science*, **5**, 117–126.

Oksanen J, Blanchet FG, Kindt R *et al.* (2015) VEGAN: *Community ecology package*. R package version 2.3-0. http://CRAN.Rproject.org/package=vegan.

Pelc RA, Warner RR, Gaines SD (2009) Geographical patterns of genetic structure in marine species with contrasting life histories. *Journal of Biogeography*, **36**, 1881–1890.

Pritchard JK, Stephens M, Donnelly P (2000) Inference of population structure using multilocus genotype data. *Genetics*, **155**, 945–959.

Puritz JB, Toonen RJ (2011) Coastal pollution limits pelagic larval dispersal. *Nature Communications*, **2**, 226. doi: 10.1038/ncomms1238

R Development Core Team (2015) R: *A language and environment for statistical computing* R Foundation for Statistical Computing, Vienna, Austria. http://www.R-project.org/.

Reed DC (1990) The effects of variable settlement and early competition on patterns of kelp recruitment. *Ecology*, **71**, 776–787.

Reed DC, Neushul M, Ebeling AW (1991) Role of settlement density on gametophyte growth and reproduction in the kelps *Pterygophora californica* and *Macrocystis pyrifera* (Phaeophyceae). *Journal of Phycology*, **27**, 361–366.

Reed DC, Amsler CD, Ebeling AW (1992) Dispersal in kelps: factors affecting spore swimming and competency. *Ecology*, **73**, 1577–1585.

Reed DC, Ebeling AW, Anderson TW, Anghera M (1996) Differential reproductive responses to fluctuating resources in two seaweeds with different reproductive strategies. *Ecology*, **77**, 300–316.

Reed DC, Anderson TW, Ebeling AW, Anghera M (1997) The role of reproductive synchrony in the colonization potential of kelp. *Ecology*, **78**, 2443–2457.

Reed DC, Schroeter SC, Raimondi PT (2004) Spore supply and habitat availability as sources of recruitment limitation in the giant kelp *Macrocystis pyrifera* (phaeophyceae). *Journal of Phycology*, **40**, 275–284.

Riginos C, Liggins L (2013) Seascape genetics: populations, individuals, and genes marooned and adrift. *Geography Compass*, **7**, 197–216.

Rousset F (1997) Genetic differentiation and estimation of gene flow from *F*-statistics under isolation by distance. *Genetics*, **145**, 1219–1228.

Rousset F (2000) Genetic differentiation between individuals. *Journal of Evolutionary Biology*, **13**, 58–62.

Rousset F (2004) *Genetic Structure and Selection in Subdivided Populations*. Princeton University Press, Princeton, New Jersey.

Rousset F (2007) Inferences from spatial population genetics. In: *Handbook of Statistical Genetics* (eds Balding DJ, Bishop M, Cannings C), pp. 945–979. John Wiley & Sons, Chichester, UK.

Roy K, Jablonski D, Valentine JW (1995) Thermally anomalous assemblages revisited: patterns in the extraprovincial latitudinal range shifts of Pleistocene marine molluscs. *Geology*, **23**, 1071–1074.

Saunders GWG (2014) Long distance kelp rafting impacts seaweed biogeography in the northeast Pacific: the kelp conveyor hypothesis. *Journal of Phycology*, **50**, 968–974.

Schiel DR, Foster MS (2015) *The Biology and Ecology of Giant Kelp Forests*. University of California Press, Oakland, California.

Selkoe KA, Toonen RJ (2011) Marine connectivity: a new look at pelagic larval duration and genetic metrics of dispersal. *Marine Ecology Progress Series*, **436**, 291–305.

Selkoe KA, Vogel A, Gaines SD (2007) Effects of ephemeral circulation on recruitment and connectivity of nearshore fish populations spanning Southern and Baja California. *Marine Ecology Progress Series*, **351**, 209–220.

Selkoe KA, Henzler CM, Gaines SD (2008) Seascape genetics and the spatial ecology of marine populations. *Fish and Fisheries*, **9**, 363–377.

Selkoe KA, Watson JR, White C *et al.* (2010) Taking the chaos out of genetic patchiness: seascape genetics reveals ecological and oceanographic drivers of genetic patterns in three temperate reef species. *Molecular Ecology*, **19**, 3708–3726.

Shchepetkin AF, McWilliams JC (2005) The regional oceanic modeling system (ROMS): a split-explicit, free-surface, topography-following-coordinate oceanic model. *Ocean Modelling*, **9**, 347–404.

Simons RD, Siegel DA, Brown KS (2013) Model sensitivity and robustness in the estimation of larval transport: a study of particle tracking parameters. *Journal of Marine Systems*, **119–120**, 19–29.

Slatkin M (1993) Isolation by distance in equilibrium and nonequilibrium populations. *Evolution*, **47**, 264–279.

Templeton AR (2006) *Population Genetics and Microevolutionary Theory*. John Wiley & Sons Inc, Hoboken, New Jersey.

Treml EA, Roberts JJ, Chao Y, Halpin PN, Possingham HP, Riginos C (2012) Reproductive output and duration of the

© 2015 John Wiley & Sons Ltd

pelagic larval stage determine seascape-wide connectivity of marine populations. *Integrative and Comparative Biology*, **52**, 525–537.
Valentine J (1966) Numerical analysis of marine molluscan ranges on the extratropical northeastern Pacific shelf. *Limnology and Oceanography*, **11**, 198–211.
Van Oosterhout C, Hutchinson WF, Wills DPM, Shipley P (2004) MICRO-CHECKER: Software for identifying and correcting genotyping errors in microsatellite data. *Molecular Ecology Notes*, **4**, 535–538.
Wang IJ, Bradburd GS (2014) Isolation by environment. *Molecular Ecology*, **23**, 5649–5662.
Waples RS, Gaggiotti O (2006) What is a population? An empirical evaluation of some genetic methods for identifying the number of gene pools and their degree of connectivity. *Molecular Ecology*, **15**, 1419–1439.
Wares JP, Gaines SD, Cunningham CW (2001) A comparative study of asymmetric migration events across a marine biogeographic boundary. *Evolution: International Journal of Organic Evolution*, **55**, 295–306.
Washburn L, Fewings MR, Melton C, Gotschalk C (2011) The propagating response of coastal circulation due to wind relaxations along the central California coast. *Journal of Geophysical Research: Oceans*, **116**, 1–16.
Watson JR, Hays CG, Raimondi PT *et al.* (2011) Currents connecting communities: nearshore community similarity and ocean circulation. *Ecology*, **92**, 1193–1200.
White C, Selkoe KA, Watson J, Siegel DA, Zacherl DC, Toonen RJ (2010) Ocean currents help explain population genetic structure. *Proceedings of the Royal Society of London B: Biological Sciences*, **277**, 1685–1694.
Wright S (1943) Isolation by distance. *Genetics*, **28**, 114–138.

M.L.J. assisted with study design, designed R code, ran models, performed statistical analyses and drafted the manuscript. F.A. designed the study, provided samples, assisted with analysis and R coding, coordinated the project and helped to draft the manuscript. D.C.R. and P.T.R. designed the study and provided the samples. N.C.C. carried out microsatellite PCR amplifications and preliminary analysis. M.A.Y., P.T.D., C.A.E., K.C., J.A., T.W.B. and D.A.S. performed spatial modelling and environmental analysis. L.B.L. assisted with preliminary analysis and provided samples. J.A.C. assisted with study design. E.A.S. assisted with study design and project coordination. All authors edited and approved the final manuscript.

Data accessibility

R scripts, microsatellite data and environmental data for all analyses: available on DRYAD (doi:10.5061/dryad.gm2v0) and through the data portal on the Santa Barbara Coastal Long Term Ecological Research Website: http://sbc.lternet.edu//data/index.html.

Supporting information

Additional supporting information may be found in the online version of this article.

Fig. S1 Best matching networks for STRUCTURE clusters and summer oceanographic transport based on adjusted Rand index.

Fig. S2 Two-factor regression model using habitat continuity and minimum transport time as independent variables to predict genetic differentiation ($F_{ST}/1 - F_{ST}$) in *Macrocystis pyrifera* in the Central California STRUCTURE cluster.

Fig. S3 Two-factor regression model using summer temperature difference and January minimum transport time as independent variables to predict genetic differentiation in the Santa Barbara Channel STRUCTURE cluster.

Fig. S4 Simple linear regression model using summer minimum transport time as an independent variable to predict genetic differentiation in the Southern California STRUCTURE cluster.

© 2015 John Wiley & Sons Ltd